Active-sensing Structural Health Monitoring via Statistical Learning: An Experimental Study under Varying Damage and Loading States

Ahmad Amer, Shabbir Ahmed, Fotis Kopsaftopoulos

Intelligent Structural Systems Laboratory (ISSL), Mechanical, Aerospace and Nuclear Engineering, Rensselaer Polytechnic Institute, Troy, NY 12180, USA
{amera2,ahmeds6,kopsaf}@rpi.edu

Abstract. Active-sensing acousto-ultrasound structural health monitoring (SHM) constitutes an important family of methods for both metallic and composite structures. However, the presence of varying operational and environmental conditions in the real world can significantly affect their accuracy and robustness in the face of uncertainty. In this context, statistical learning methods that can be based on Gaussian Process regression models (GPRMs) and statistical time-series models can be incorporated in the damage diagnostic process to account for and properly represent such uncertainties. Towards this end, the main objective of this paper is the postulation and experimental assessment of two statistical learning approaches, based on GPRMs and time-varying time series models, for active sensing SHM under varying structural and loading states under uncertainty. The proposed methods involve GRPM representation of the non-linear mapping between the actual state with (i) traditional damage indices (DIs) and (ii) parameters of time-dependent autoregressive (TAR) models. The experimental validation and comparative assessment is based on a series of experiments on an aluminum coupon outfitted with a network of piezoelectric actuators/sensors subjected to different static loads under increasing damage size.

Keywords: active sensing · · structural health monitoring · guided waves · Gaussian Process regression models · time series models

1 Introduction

For the majority of engineering structural systems, operational complexity, as manifests in multiple and varying operating and environmental conditions, poses as the major challenge for currently-employed structural health monitoring (SHM) technologies. In the field of active-sensing guided-wave SHM, most of the proposed state-of-the-art approaches, such as health/damage indicators, are of deterministic nature, i.e. they do not account for operating, environmental and modeling uncertainties [8, 3, 2]. This limitation oftentimes leads to the lack of accuracy and robustness in the face of stochastic time-varying and non-linear structural responses, such as those originating from reflections from boundary

conditions as well as complex damage types that can be easily masked by the effects of varying operational and environmental conditions [19, 18].

Towards this end, guided-wave SHM under varying operational and environmental conditions has to properly consider the effects of varying conditions on wave propagation signals [8]. Two widely-used approaches comprise the families of baseline-free [14] and compensation techniques (see for instance [16]). Although these techniques have shown promising results in marginalizing the undesired effects, they are facing challenges related to limited applicability to simple boundary conditions and confinement to the range of studied conditions [2]. This stems from the lack of proper modeling of the short and long-term effects of operational and environmental conditions [5]. On the modeling side, time series models have been extensively used in representing the dynamic response of structures under operational and environmental uncertainty, as well as time-varying effects within the context of vibration-based SHM (see for instance [6, 13, 10]. However, such approaches may face challenges when substantial experimental uncertainty, such as that coming from varying conditions, is present, as evident by the low type I error probability level that is oftentimes required to compensate for this [11]. In addition, lack of robustness against new or unknown sources of uncertainty that may not be involved in the initial model is an additional challenge that has to be addressed [5]. As active-sensing guided-wave SHM methods are prone to many sources of uncertainty (such as sensor position, adhesive properties, damage propagation patterns) [9], the task of migrating these models into the realm of guided-wave SHM is not be straight-forward. In this context, Gaussian Process (GP) models have been used for vibration-based SHM in order to model uncertainty in system response [7]. One of the advantages of this approach is the flexibility in modeling both known and unknown sources of uncertainty. In particular, the integration of time series and Gaussian Process models [20, 5] has shown promise in modeling non-linear dynamics, as well as system response under different sources of variation.

In recent studies, the authors investigated the use of Gaussian Process regression models (GPRMs) for probabilistic damage quantification in guided-wave SHM [3, 4]. Also, GPRMs and time-varying times series models were recently used by the authors for aircraft state awareness within complex dynamic environments under varying flight states [1]. Building upon previous work, the objective of this study is the postulation and experimental validation and assessment of two statistical learning approaches, based on GPRMs and time-varying time series models, for active sensing SHM under varying structural and loading states in the face of uncertainty. The proposed methods are based on the GRPM representation of the non-linear mapping between the actual structural and loading state with (i) traditional damage indices (DIs) and (ii) parameters of identified time-dependent autoregressive (TAR) models. To the authors' best of knowledge, this is the first time such a framework is applied to tackle probabilistic active-sensing SHM. In the first method, GPRMs are used to model the evolution of a state-of-the-art DI with increasing damage size and load. In the second, TAR models are used to represent the time-varying wave propagation

signals between the actuator-sensor paths and GPRMs are used to model the relationship of TAR parameters with damage, load, and time, thus providing a unified framework for modeling non-stationary wave propagation and damage quantification under varying structural and load conditions.

2 Background

2.1 Gaussian Process Regression Models

Formulation Briefly, given a training data set $\mathcal{D}$ containing n inputs-observation pairs $\{(\mathbf{x}_i \in \mathbb{R}^D, y_i \in \mathbb{R},\ i = 1, 2, 3, \ldots, n\}$, a GPRM can be formulated as [15]:

$$y = f(\mathbf{x}) + \epsilon \tag{1}$$

where a GP prior with mean $m(\mathbf{x})$ and covariance $k(\mathbf{x}, \mathbf{x}')$ is placed on the latent function $f(\mathbf{x})$, and an independent, identically-distributed (*iid*), zero-mean Gaussian prior with variance σ_n^2 is placed on the noise term ϵ, that is:

$$f(\mathbf{x}) \sim \mathcal{GP}(m(\mathbf{x}), k(\mathbf{x}, \mathbf{x}')),\ \ \epsilon \sim iid\, \mathcal{N}(0, \sigma_n^2) \tag{2}$$

where $\mathcal{N}(\cdot, \cdot)$ indicates normal distribution with the indicated mean and variance. As is common in the GPRM literature, $m(\mathbf{x})$ can be set to zero and the squared exponential covariance function (kernel) is used for the latent function GP [15].

Training Training of the GPRM involves optimizing the hyperparameters θ of the covariance function, including σ_n^2 and the input/output length scales, which is typically implemented *via* Type II Maximum Likelihood [15, Chapter 5, pp. 109], whereas the marginal likelihood (evidence) of the training observations is maximized (or its negative log is minimized). That is:

$$-\log p(\mathbf{y}|X, \theta) = -\log \mathcal{N}(\mathbf{y}|\mathbf{0}, K_{XX} + \sigma_n^2 \mathbb{I}) \tag{3a}$$

$$= -\frac{1}{2}\mathbf{y}^T (K_{XX} + \sigma_n^2 \mathbb{I})^{-1}\mathbf{y} - \frac{1}{2}\log |K_{XX} + \sigma_n^2 \mathbb{I}| - \frac{n}{2}\log 2\pi \tag{3b}$$

with K_{XX} denoting the covariance matrix of the training input data X, and $\mathbb{I}$ the identity matrix.

Prediction Prediction is based on the assumption of joint Gaussian distribution between the training observations $\mathbf{y}$ and a test observation (to be predicted) of the test input set $(\mathbf{x}_*)$ as follows [15]:

$$\begin{bmatrix} \mathbf{y} \\ y_* \end{bmatrix} = \mathcal{N}\left[\mathbf{0}, \begin{matrix} K_{XX} + \sigma_n^2 \mathbb{I} & \mathbf{k}_{X\mathbf{x}_*} \\ \mathbf{k}_{\mathbf{x}_* X} & k_{\mathbf{x}_*\mathbf{x}_*} + \sigma_n^2 \mathbb{I} \end{matrix}\right] \tag{4}$$

In the above expression, $\mathbf{k}_{\mathbf{x}_* X}$ is the vector of covariances between the set of test inputs $\mathbf{x}_*$ and training input matrix X, and $k_{\mathbf{x}_*\mathbf{x}_*}$ is the scalar variance of the set of test inputs. The predictive distribution over $\mathbf{y}_*$ can then be defined as follows:

$$p(y_*|\mathbf{x}_*, X, \mathbf{y}) = \mathcal{N}(\mathbb{E}\{y_*\}, \mathbb{V}\{y_*\}), \qquad \text{with} \tag{5a}$$

$$\mathbb{E}\{y_*\} = \mathbf{k}_{\mathbf{x}_* X}(K_{XX} + \sigma_n^2 \mathbb{I})^{-1}, \mathbb{V}\{y_*\} = k_{\mathbf{x}_*\mathbf{x}_*} - \mathbf{k}_{\mathbf{x}_* X}(K_{XX} + \sigma_n^2 \mathbb{I})^{-1}\mathbf{k}_{X\mathbf{x}_*} + \sigma_n^2 \tag{5b}$$

such that $\mathbb{E}\{\cdot\}$ and $\mathbb{V}\{\cdot\}$ are the mean and variance functions, respectively.

2.2 Adaptive time-dependent AR models

Guided waves are inherently non-stationary due to their time-dependent (evolutionary) characteristics and heavily influenced by environmental and operating conditions. The time-varying nature of wave propagation requires the use of corresponding time-varying non-parametric and/or parametric models [13, 17, 12]. Stochastic parametric non-stationary (time-varying) models such as time-dependent autoregressive (TAR) models or related types and their extensions have been mainly used in the context of random vibration analysis [13, 17, 12], with a detailed review presented in [13]. In this study, the time-varying characteristics of the guided wave propagation signals between actuator-sensor paths of the sensor network under the influence of varying operating and structural health states have been modeled via TAR models. TAR models represent their conventional, stationary AR counterparts with the significant difference being that they allow their parameters to depend upon time and *adapt* based on the time-dependent nature of the wave propagation [13, 17]. A TAR(na) model, with na designating its AR order, is thus of the form:

$$y[t] + \sum_{i=1}^{na} a_i[t] \cdot y[t-i] = e[t] \quad \text{with} \quad e[t] \sim \text{iid}\, \mathcal{N}\big(0, \sigma_e^2[t]\big) \tag{6}$$

with t designating discrete time, $y[t]$ the time-varying wave propagation signal to be modeled, $e[t]$ an (unobservable) uncorrelated (white) innovations sequence with zero mean and time-dependent variance $\sigma_e^2[t]$, and $a_i[t]$, the model's time-dependent AR parameters.

Non-stationary TAR model identification Given a single, N-sample-long, non-stationary signal record $\{y[1], \ldots, y[N]$, the TAR identification problem may be stated as the problem of selecting the corresponding model structure and estimating the model parameters $a_i[t]$ and the innovations variance $\sigma_e^2[t]$ that "best" fit the available measurements. The TAR model is parameterized via the AR parameter vector $\boldsymbol{\theta}[t] = [a_1[t]\ a_2[t]\ \ldots\ a_{na}[t]]^T_{(na\times 1)}$ to be estimated based on the recorded non-stationary signal. The model identification problem is usually distinguished into two subproblems: (i) *parameter estimation* and (ii) *model structure selection*. For a detailed review of parameter estimation and model structure selection methods see [13, 12]. In this work, parameter estimation is based on an exponentially weighted prediction error criterion (incorporating a "forgetting" factor [13]) and a recursive estimation scheme accomplished via the recursive maximum likelihood (RML) method [13, 12].

3 The Experimental Setup and the Signals

In this study, a 152.4 × 279.4 mm (6 × 11 in) 6061 aluminum coupon (2.36 mm/0.093 in thick) was used (Figure 1a). Using Hysol EA 9394 adhesive, 6 lead zirconate titanate (PZT) piezoelectric sensors (type PZT-5A, Acellent Technologies, Inc) of 3.175 mm (1/8 in) diameter and a thickness of 0.2 mm (0.0079 in),

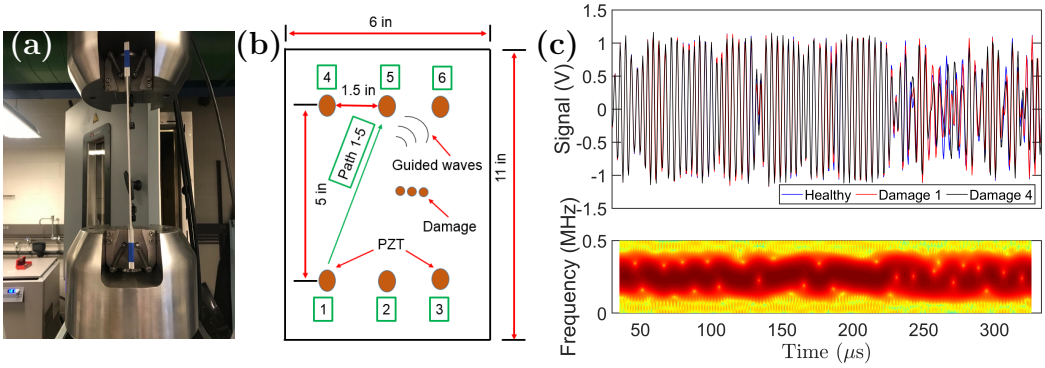

Fig. 1. (a) The plate used in this study installed on the testing machine; (b) a schematic of the plate's sensor layout and dimensions; (c) realization of the guided wave signal for healthy and damaged cases with a representative non-parametric spectrogram analysis.

were attached to the plate and cured under vacuum for 24 hrs in room temperature. Figure 1b shows the dimensions of the plate, placement of the PZT transducers and the path naming convention. After curing, the plate was mounted on a tensile testing machine (Instron, Inc), where five static loading conditions were applied consecutively: 0, 5, 10, 15 and 20 kN. During each loading phase, up to four three-gram weights were taped to the surface of the plate starting from its center-point to simulate local damage (Figure 1b).

Actuation signals in the form of 5-peak tone bursts (5-cycle Hamming-filtered sine wave, 90 V peak-to-peak, 250 kHz center frequency) were generated in a pitch-catch configuration over each sensor consecutively. Data was collected using a ScanGenie III data acquisition system (Acellent Technologies, Inc) from selected sensors during each actuation cycle at a sampling frequency of 24 MHz. Using this process, 20 signals for each sensor (wave propagation path), damage, and loading condition were recorded, with the exception of the case of 20 kN, where only 2 data sets were recorded per damage state. This lead to a total of 410 data sets for each sensor. For the time-series modeling, the acquired signals were down-sampled to 2 MHz. This resulted in 612-sample-long signals for the TAR-based analysis. Figure 1c presents indicative non-parametric results[1] in the form of the wave spectrogram that shows the time-varying nature of the wave propagation signal.

4 DI-trained GPRM Results

For the first method proposed in this study, GPRMs were trained using the values of a conventional DI formulation as developed in [9]. For a specific signal path, 500 DI values were randomly selected out of the 8,000 available data points and used as the training output, while the damage size and load states were used as inputs. In the said format, the trained GPRMs are capable of predicting DI values and their distribution based on an input vector that contains the

[1] window length: 30 samples; 98% overlap; NFFT points: 30000 (zero-padding took place to obtain smooth magnitude estimates); frequency resolution $\Delta f = 666.66$ Hz.

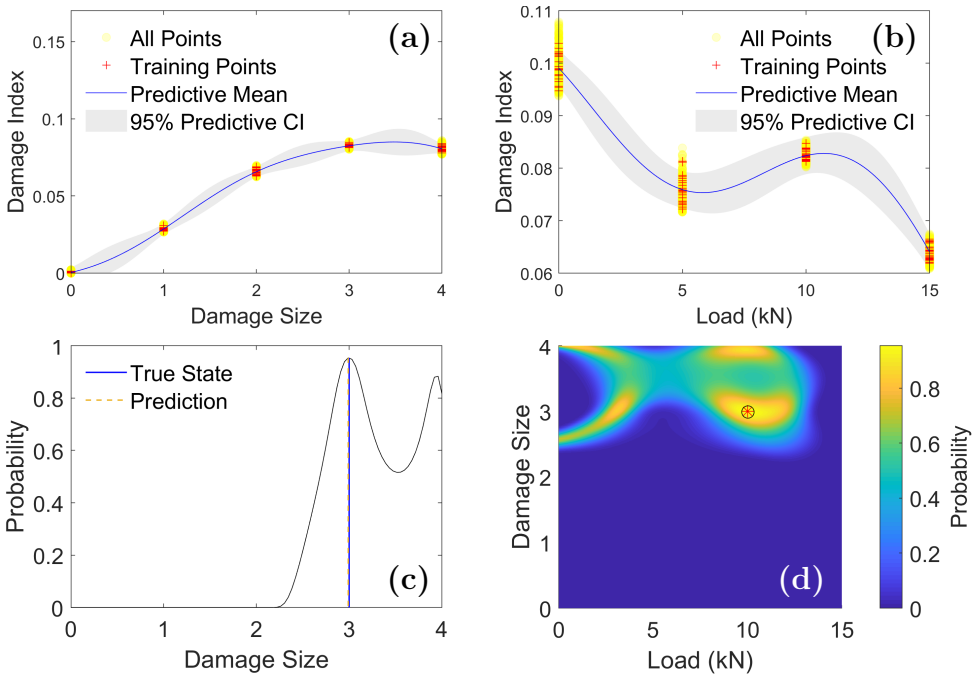

Fig. 2. Two-input DI-based GPRMs and their prediction capabilities. (a) A GPRM modeling DI *vs* damage size at a load of 10 kN. (b) A GPRM modeling DI *vs* load at a damage size of 3 weights. (c) State prediction capability of the GPRM in (a) in the case the load was known. (d) State Prediction probability in case neither the load nor the damage size is known. The red asterisk indicates the true state, while the black circle indicates the point of maximum probability.

structural state, i.e. damage size and load. during inspection, as DI values are available instead of states, the actual state of the structure can be predicted using the trained GPRM and (i) calculating the predictive confidence interval (CI) at the test/validation DI values, and (ii) calculating the probability that a point sampled from the predictive distribution of each set of states (damage size and load) would fall within the calculated CIs. The damage size and load that show the highest probability would be identified as the actual state corresponding to the observed test/validation DI value.

Figure 2 shows an indicative example of a GPRM that represents the mapping between two inputs, namely damage size and load, and one output, that is the DI. As shown in panels a and b, the model is able to capture the evolution of the DI with damage and load, respectively. This is also evident in the model's overall mean squared error (MSE) of $2.81 \cdot 10^{-}6$ and normalized residual sum of squares (RSS/SSS) of 0.085%, both based on the validation (test) data set not used for training. When it comes to state estimation, if the load is assumed to be known, as might be the case in some practical situations, the model can accurately predict the damage size, as shown in Figure 2c. Furthermore, because this is a two-input model, the GPRM also accurately predicts both damage size

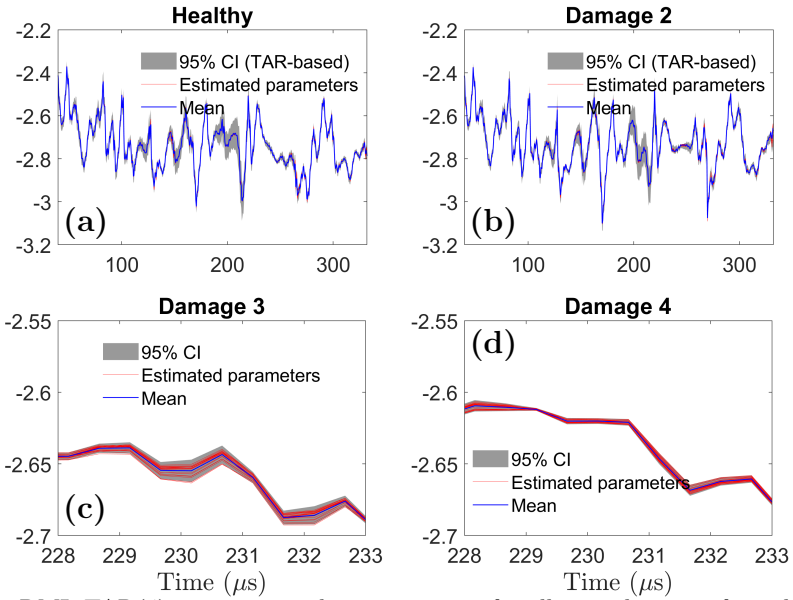

Fig. 3. RML-TAR(4)$_{0.835}$ estimated a_1 parameters for all 20 realizations for indicative damage states, namely: (a) healthy; (b) damage state 2 (set load at 0 kN) with corresponding 95% TAR-based confidence intervals; (c) close-up of the RML-TAR(4)$_{0.835}$ estimated a_1 parameters for damage state 3 and (d) damage state 4 (set load at 0 kN). The 95% confidence intervals are derived from 20 realizations of the model parameters.

and load, if both states are assumed to be unknown, as presented in Figure 2d. These results are a preliminary demonstration of the effectiveness of the DI-trained GPRMs to tackle damage quantification under varying loads within a probabilistic framework.

5 TAR-trained GPRM Results

The parametric identification of the wave propagation signals is achieved via TAR models based on 612 (332 μs) sample-long response signals (sampling frequency f_s = 2 MHz) recorded via embedded piezoelectric sensors. The model order and forgetting factor estimation, i.e. the model "structure" selection problem, is based on the successive estimation of TAR(na) models for orders $na = 2, \ldots, 22$ and forgetting factors $0.500, \ldots, 0.999$ with an increment of 0.001 with the best model selected based on the combined consideration of the Bayesian Information Criterion (BIC), RSS/SSS criterion [13] and the comparison with the corresponding non-parametric spectral estimates. This process resulted in a final model of order na = 4 and forgetting factor 0.835, designated as RML-TAR(4)$_{0.835}$, for representing the non-stationary wave propagation signal.

Figure 3a and b show the estimated time-dependent a_1 model parameters for indicative damage states, namely for the healthy and damage state 2 (two added weights), respectively. In Figure 3 the 20 estimated parameters a_1 for the healthy (Figure 3a) and damage 2 case (Figure 3b) are shown in red with the

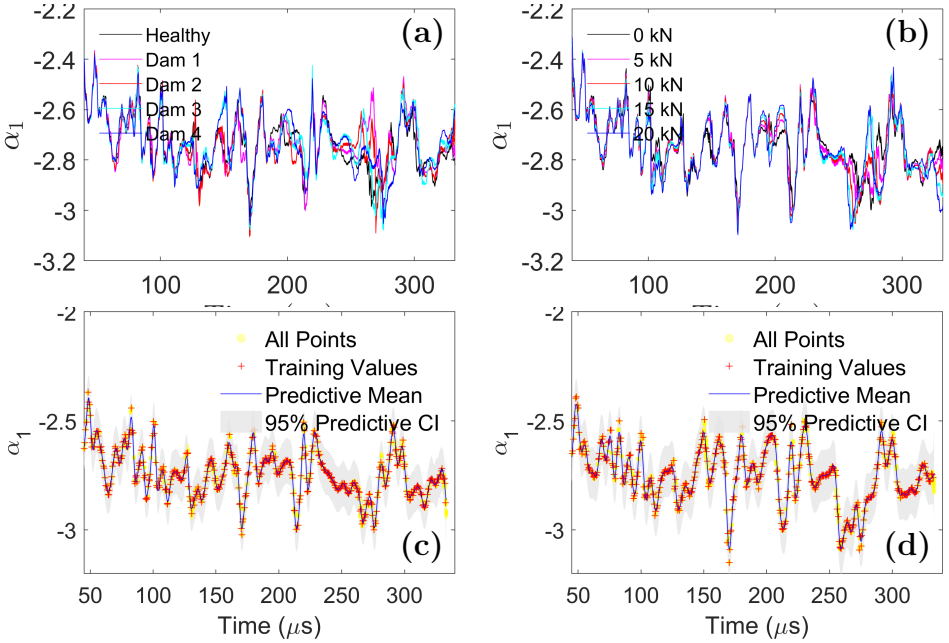

Fig. 4. RML-TAR(4)$_{0.835}$ parameter a_1 for all 20 realizations of different states: (a) all damage states (set load at 0 kN); (b) all load levels (set damage state as healthy); (c) GPRM-based results of the first RML-TAR(4)$_{0.835}$ parameter a_1 for the healthy structure under 0 kN; (d) GPRM-based results of the first RML-TAR(4)$_{0.835}$ parameter a_1 for damaged structure (4 added weights) under 15 kN.

corresponding sample mean shown in blue. The grey shaded region represents the 95% confidence interval which has been derived from a single RML-TAR(4)$_{0.835}$ model obtained from a single wave signal from the corresponding state. It is significant to note that the confidence interval derived from a single realization is able to capture the variation of all 20 time-dependent model parameters. It can also be observed that at 213.2 μs, the confidence interval is higher than all other time instants. Figure 3c and d show the magnified view of the model parameter a_1 for a shorter time range for indicative damage states, namely damage 3 and 4 for a set load of 0 kN. The red lines represent all 20 estimates of the TAR a_1 parameters, the blue line represents their sample mean and the grey shaded region represent the 95% confidence interval derived from the 20 estimated parameters. Similar trends are observed in the case of TAR models under different loads and set damage, but are omitted for the sake of brevity.

TAR models allow for the modeling of time-varying wave propagation signals. However, based on the current formulation, multiple TAR models have to be identified for multiple damage and load states. Figure 4a and b present the RML-TAR(4)$_{0.835}$ a_1 time-dependent parameters as estimated for the considered structural health and load states, respectively. Observe the non-uniform time variation of the estimated parameters for the considered states. In this context, GPRMs are proposed to model the evolution of the TAR model parameters with time, damage size and load in order to negate the need for a multi-model

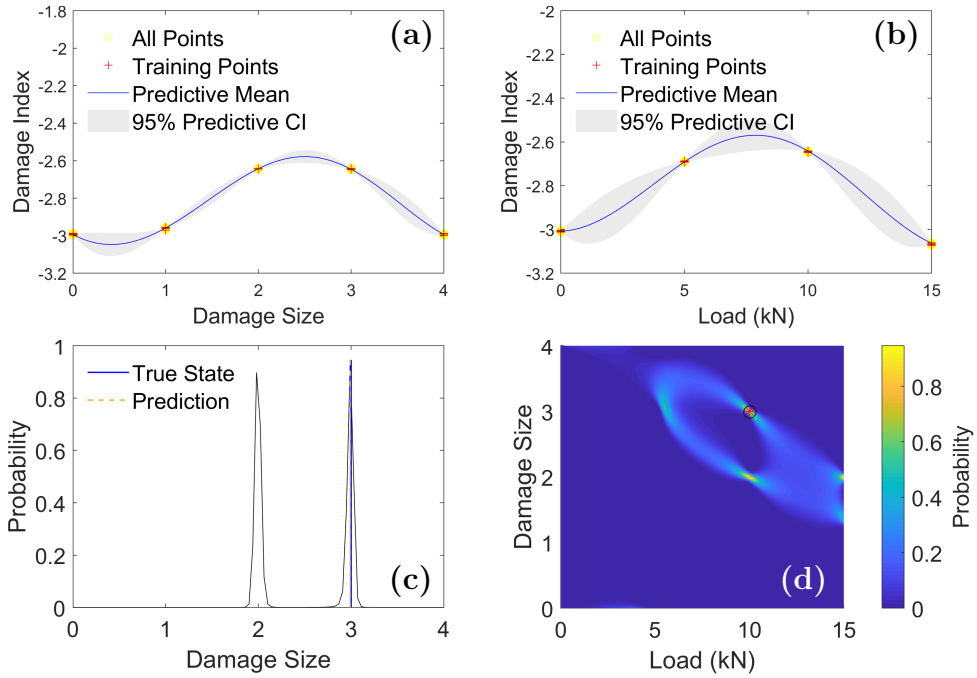

Fig. 5. Two-input parameter-based GPRMs and damage state prediction results: (a) GPRM modeling the first RML-TAR(4)$_{0.835}$ parameter *vs* damage size at set load of 10 kN; (b) GPRM modeling the first parameter *vs* load at a damage size of 3 weights; (c) GPRM-based damage size prediction when load is known; (d) state prediction probability in case neither the load nor the damage size is known. The red asterisk indicates the true state while the black circle indicates the point of maximum probability.

approach. Initially, GPRMs were trained using single-state TAR model parameters to model their evolution with time allowing for improved representation of experimental uncertainty compared to the TAR-based parameter covariance matrix. Towards this end, 500 points out of 61, 200 samples were used for training and the rest were used for validation. Figure 4c and d show indicative GPRM results for the first parameter in the TAR model in the healthy under 0 kN case and the 4-weight damage under 15 kN case, respectively.

After modeling the evolution of parameters with time, the second step in integrating GPRMs with TAR models under different states was to model the evolution of the parameters under the considered damage and load states. In this case, specific time instants of interest (such as those where the parameters are most affected by damage and/or load) were chosen for GP modeling. Two-input GPRMs were trained with the values of the model parameters at the selected time instants (model output) under varying damage and load conditions (model inputs). Figure 5 shows the indicative results of the first parameter GPRM at precisely 259.1116 μs, trained with 200 (out of 400) data points with an MSE of $2.52 \cdot 10^{-5}$ and an RSS/SSS of 0.0003%. Again, the model accurately follows the first parameter of the RML-TAR(4)$_{0.835}$ model with damage size and load, as

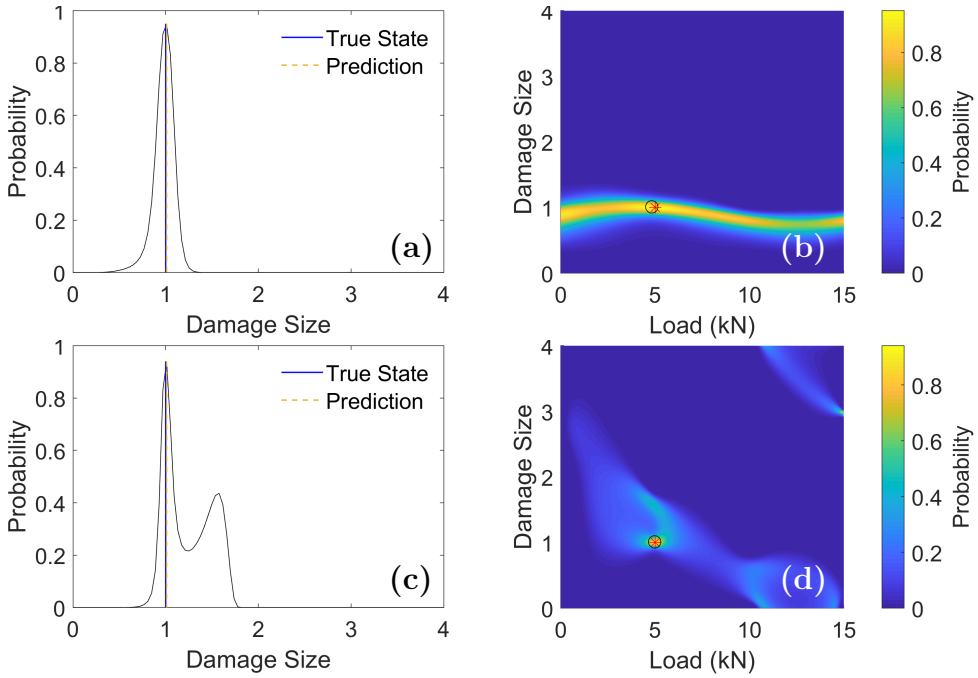

Fig. 6. Comparison of prediction performance of DI-based and parameter-based GPRMs: (a) DI-based GPRM damage size prediction with known load ; (b) DI-based GPRM 2-state prediction when neither load nor damage size is known; (c) Parameter-based GPRM damage size prediction with known load; (d) Parameter-based GPRM 2-state prediction in case neither load nor damage size is known. The red asterisk indicates the true state, while the black circle indicates the point of maximum probability.

shown in Figure 5a and b, respectively. These results are useful in estimating in a time-efficient manner the value of the parameter under different states without the need to identify multiple TAR models. When it comes to predicting the structural state based on the estimated TAR parameter value, assuming the load is known, the model accurately predicts damage size as shown in Figure 5c and accurately predicts both damage size and load, when both are assumed unknown (Figure 5d).

One interesting observation pertains to the difference between the prediction plots of the RML-TAR$(4)_{0.835}$ parameter-based GPRMs in Figure 5c and d, and those of the DI-based GPRM in Figure 2c and d. In both cases, the same load and damage size are predicted from the trained models, and both models perform effectively. However, in the parameter-based GPRM, the 1-state prediction (see Figure 5c) is sharper than that of the DI-based GPRM. In addition, the 2-state prediction (Figure 5d) indicates the areas of high probability that are confined to two main regions, compared to the broader distribution of the prediction probability in the DI-trained GPRM of Figure 2d. This behaviour is consistent with multiple damage and load states. Figure 6 shows the predictions of both models for another indicative set of damage and load states where the sharpness of the parameter-based GPRM 2-state prediction in Figure 6d is even more

evident compared to its DI-based counterpart (Figure 6b), which exhibits a strip of high probability spanning a set damage size across all load states. This exemplifies the advantages of the modeling approach in the TAR-trained GPRM framework over conventional approaches that can be further enhanced with the inclusion of the complete time evolution of the model parameters.

6 Conclusions

In this work, two statistical learning approaches, based on GPRMs and time-varying time series models, for active sensing SHM under varying damage and loading states were presented and experimentally assessed. The proposed methods are based on the GRPMs: (i) GPRMs were used to model the evolution of a conventional DIs with increasing damage size and load, and (ii) RML-TAR models were used to represent the time-varying wave propagation signals between the actuator-sensor paths and integrated with GPRMs to map the relationship between TAR parameters and the structural state. Both approaches showed perfect damage size prediction when the load was assumed to be known. However, for two-state prediction, that is assuming both the damage size and load to be unknown, the TAR-trained GPRMs showed a more focused, and thus accurate prediction of the true structural state compared to the DI-trained GPRMs as indicated by the results obtained from validation data.

7 Acknowledgments

This work was supported by the U.S. Air Force Office of Scientific Research (AFOSR) grant "Formal Verification of Stochastic State Awareness for Dynamic Data-Driven Intelligent Aerospace Systems" (FA9550-19-1-0054) and Program Officer Dr. Erik Blasch, as well as the Army/Navy/NASA Vertical Lift Research Center of Excellence (VLRCOE) Program, grant number W911W61120012, with Dr. Mahendra Bhagwat and Dr. William Lewis as Technical Monitors.

References

1. Ahmed, S., Amer, A., Varela, C., Kopsaftopoulos, F.P.: Data driven state awareness for fly-by-feel aerial vehicles via adaptive time series and gaussian process regression models. In: Proceedings of the InfoSymbiotics/DDDAS2020 Conference. Springer (2020)
2. Ahmed, S., Kopsaftopoulos, F.P.: Investigation of broadband high-frequency stochastic actuation for active-sensing shm under varying temperature. In: Proceedings of the 12th International Workshop on Structural Health Monitoring (IWSHM 2019). Palo Alto, CA, USA (September 2019)
3. Amer, A., Kopsaftopoulos, F.P.: Probabilistic damage quantification *via* the integration of non-parametric time-series and gaussian process regression models. In: Proceedings of the 12th International Workshop on Structural Health Monitoring (IWSHM 2019). pp. 2384–2393. Palo Alto, CA, USA (September 2019)
4. Amer, A., Kopsaftopoulos, F.P.: Towards unified probabilistic rotorcraft damage detection and quantification via non-parametric time series and gaussian process regression models. In: Proceedings of the Vertical Flight Society 76th Annual Forum & Technology Display. Virginia Beach, VA, USA (October 2020)

5. Avendaño-Valencia, L.D., Chatzi, E.N., Koo, K.Y., Brownjohn, J.M.: Gaussian process time-series models for structures under operational variability. Frontiers in Built Environment **3**, 69 (2017)
6. Fassois, S.D., Kopsaftopoulos, F.P.: Statistical time series methods for vibration based structural health monitoring. In: Ostachowicz, W., Guemes, A. (eds.) New Trends in Structural Health Monitoring, chap. 4, pp. 209–264. Springer (2013)
7. Gonzaga, P., Dervilis, N., Worden, K., Barthorpe, R., Stevanovic, N., Bernhammer, L.: Structural health monitoring: A review of uncertainty quantification methods in wind turbine systems. In: Proceedings of the 12th International Workshop on Structural Health Monitoring (IWSHM 2019). Palo Alto, CA, USA (September 2019)
8. Gorgin, R., Luo, Y., Wu, Z.: Environmental and operational conditions effects on lamb wave based structural health monitoring systems: A review. Ultrasonics **105**, 106114 (2020)
9. Janapati, V., Kopsaftopoulos, F., Li, F., Lee, S., Chang, F.K.: Damage detection sensitivity characterization of acousto-ultrasound-based structural health monitoring techniques. Structural Health Monitoring **15**(2), 143–161 (2016)
10. Kopsaftopoulos, F., Fassois, S.D.: Vibration based health monitoring for a lightweight truss structure: experimental assessment of several statistical time series methods. Mechanical Systems and Signal Processing **24**, 1977–1997 (2010)
11. Kopsaftopoulos, F., Nardari, R., Li, Y.H., Chang, F.K.: A stochastic global identification framework for aerospace structures operating under varying flight states. Mechanical Systems and Signal Processing **98**, 425–447 (2018)
12. Ljung, L.: System identification. Wiley encyclopedia of electrical and electronics engineering pp. 1–19 (1999)
13. Poulimenos, A., Fassois, S.: Parametric time-domain methods for non-stationary random vibration modelling and analysis—a critical survey and comparison. Mechanical systems and signal processing **20**(4), 763–816 (2006)
14. Qiu, J., Li, F., Abbas, S., Zhu, Y.: A baseline-free damage detection approach based on distance compensation of guided waves. Journal of Low Frequency, Vibration and Active Control **38**, 1132–1148 (2019)
15. Rasmussen, C.E., Williams, C.K.I. (eds.): Gaussian Processes for Machine Learning. MIT Press (2006)
16. Roy, S., Ladpli, P., Chang, F.K.: Load monitoring and compensation strategies for guided-waves based structural health monitoring using piezoelectric transducers. Journal of Sound and Vibration **351**, 206–220 (2015)
17. Sotiriou, D., Kopsaftopoulos, F., Fassois, S.: An adaptive time-series probabilistic framework for 4-d trajectory conformance monitoring. IEEE Transactions on Intelligent Transportation Systems **17**(6), 1606–1616 (2016)
18. Spiridonakos, M., Fassois, S.: Non-stationary random vibration modelling and analysis via functional series time-dependent arma (fs-tarma) models–a critical survey. Mechanical Systems and Signal Processing **47**(1-2), 175–224 (2014)
19. Wilson, C.L., Lonkar, K., Roy, S., Kopsaftopoulos, F., Chang, F.K.: Structural health monitoring of composites. In: Beaumont, P.W.R., Zweben, C.H. (eds.) Comprehensive Composite Materials II, pp. 382–407. Elsevier Ltd. (2018)
20. Worden, K., Rogers, T., Cross, E.: Identification of nonlinear wave forces using gaussian process narx models. In: Kerschen, G. (ed.) Nonlinear Dynamics, Volume 1. Conference Proceedings of the Society for Experimental Mechanics Series. Springer (2017)